

Dynamic, Self-Calibrating, Threshold-Detecting, Differential Speed and Direction Hall-Effect Gear Tooth Sensor

Features and Benefits

- Rotational direction detection
- High start-up and running mode vibration immunity
- Single-chip sensing IC for high reliability
- Internal current regulator for two-wire operation
- Variable pulse width output protocol
- Automatic Gain Control (AGC) and offset adjust circuit
- True zero-speed operation
- Wide operating voltage range
- Undervoltage lockout
- ESD and reverse polarity protection

Package: 4-pin SIP Module (suffix SH)



Not to scale

Description

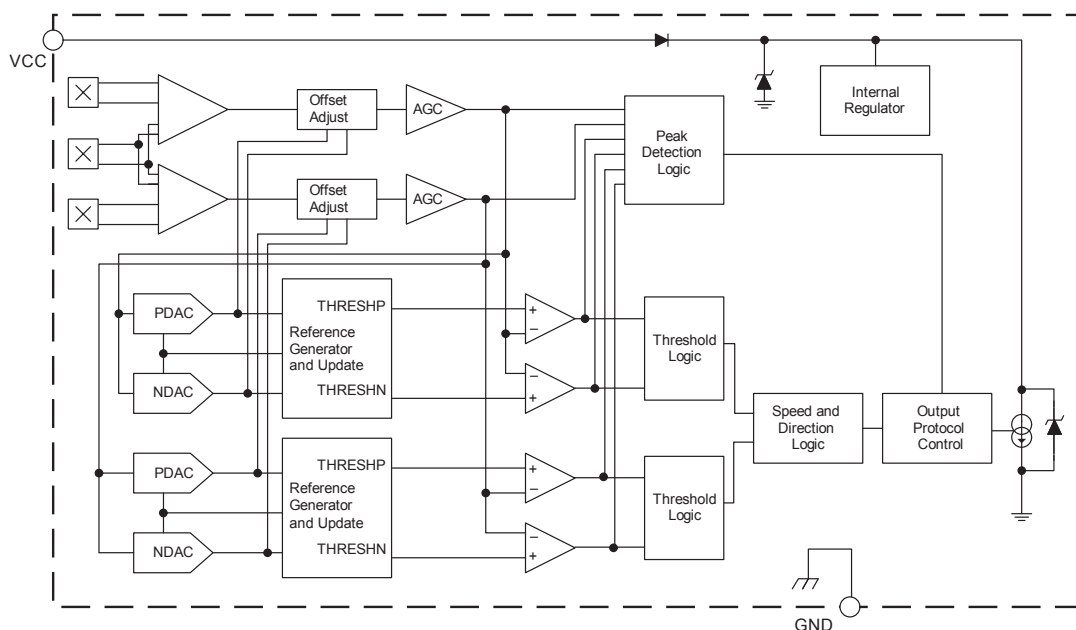
The ATS657 includes an optimized Hall-effect sensing integrated circuit (IC) and magnet to create a user-friendly solution for direction detection and true zero-speed, digital gear tooth sensing in two-wire applications. The small package can be easily assembled and used in conjunction with a wide variety of gear tooth sensing applications.

The IC employs patented algorithms for the special operational requirements of automotive transmission applications. The speed and direction of the target are communicated by this two-wire device through a variable pulse width output protocol. The advanced vibration detection algorithm systematically calibrates the sensor on the initial teeth of a true rotation signal and not on vibration, always guaranteeing an accurate signal in running mode. Even the high angular vibration caused by engine cranking is completely rejected by the device.

Patented running mode algorithms also protect against air gap changes whether or not the target is in motion. Advanced signal processing and innovative algorithms make the ATS657 an ideal solution for a wide range of speed and direction sensing needs.

The device package is lead (Pb) free, with 100% matte tin leadframe plating.

Functional Block Diagram



Selection Guide

Part Number	Packing*
ATS657LSHTN-T	800 pieces per 13-in. reel

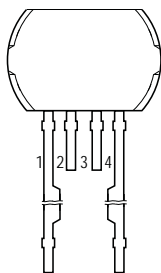
*Contact Allegro® for additional packing options



Absolute Maximum Ratings

Characteristic	Symbol	Notes	Rating	Unit
Supply Voltage	V_{CC}	See Power Derating curve; proper operation at $V_{SUPPLY} = 24\text{ V}$ requires circuit configuration with a series $100\ \Omega$ load resistor. Please refer to figure 7. Voltage between pins 1 and 4 of greater than 22 V during target rotation from pin 1 to pin 4 may partially turn on the ESD protection Zener diode in the IC.	24	V
Reverse Supply Voltage	V_{RCC}		-18	V
Operating Ambient Temperature	T_A	Range L	-40 to 150	°C
Maximum Junction Temperature	$T_J(\text{max})$		165	°C
Storage Temperature	T_{stg}		-65 to 170	°C

Pin-out Diagram



Terminal List

Number	Name	Function
1	VCC	Connects power supply to chip
2	NC	No connection
3	NC	No connection
4	GND	Ground terminal

ELECTRICAL CHARACTERISTICS Valid over operating voltage and temperature ranges, unless otherwise noted

Characteristics	Symbol	Test Conditions	Min.	Typ. ¹	Max.	Unit ²
Supply Voltage	V_{CC}	Operating, $T_J < T_{J(max)}$	4.0	–	18	V
Undervoltage Lockout	$V_{CC(UV)}$	$V_{CC} = 0 \rightarrow >4 \text{ V}$, or $>4 \rightarrow 0 \text{ V}$	–	3.5	4.0	V
Reverse Supply Current	I_{RCC}	$V_{CC} = -18 \text{ V}$	–	–	-10	mA
Supply Zener Clamp Voltage	$V_{Z(SUPPLY)}$	$I_{CC} = I_{CC(max)} + 3 \text{ mA}$, $T_A = 25^\circ\text{C}$	24.0	–	–	V
Supply Zener Resistance	R_Z		–	<5	–	Ω
Supply Current	$I_{CC(LOW)}$	Low-current state (Running mode)	5.0	6.5	8.0	mA
	$I_{CC(HIGH)}$	High-current state (Running mode)	12	14.0	16	mA
	$I_{CC(SU)(LOW)}$	Startup current level and Power-On mode	5.0	7.0	8.5	mA
	$I_{CC(SU)(HIGH)}$	High-current state (Calibration)	12	14.5	16.5	mA
Current Level Difference	ΔI_{CC}	$I_{CC(HIGH)} - I_{CC(LOW)}$	5	–	–	mA
Power-On Characteristics³						
Power-On Time	t_{on}	Speed < 200 Hz	–	–	2.0	ms
Initial Calibration						
First Output Pulse with Direction ⁴	N_{DIR}	Speed < 200 Hz, constant rotation direction	–	–	6	Edge
First Output Pulse ⁵	N_{NONDIR}	Speed < 200 Hz, constant rotation direction	–	–	2	Edge
AGC Disable	N_f	Speed < 200 Hz, constant rotation direction	–	–	5	Edge
Vibration Check	$N_{VIBCHECK}$	Speed < 200 Hz, after AGC disable	–	3	–	Edge
Time Until Correct Direction Output on High-Speed Startup	t_{HIGHSU}	10 kHz startup, $B = 300 \text{ G}_{pk-pk}$	–	5	–	ms
Running Mode Calibration⁶						
Non-Direction Pulse Output on Direction Change	$N_{BLANKDC}$	Running mode, direction change	–	1	2	Pulse
First Direction Pulse Output on Direction Change	N_{DC}	Running mode, direction change	–	2	3	Pulse
DAC Characteristics						
Allowable User-Induced Differential Offset ⁷	$B_{DIFFEXT}$		–	± 60	–	G
Output Stage						
Output Slew Rate	SR_{OUT}	$R_L = 100 \Omega$, $C_L = 10 \text{ pF}$	7	12.0	–	mA/ms

¹Typical data is at $V_{CC} = 8 \text{ V}$ and $T_A = +25^\circ\text{C}$. Performance may vary for individual units, within the specified maximum and minimum limits.

²1 G (gauss) = 0.1 mT (millitesla).

³Power-On Time is the time required to complete the initial internal automatic offset adjust; the DACs are then ready for peak acquisition.

⁴Direction of the first output pulse on the 6th edge may not be correct when undergoing vibration.

⁵Non-direction pulse output only. See figure 3 for more details.

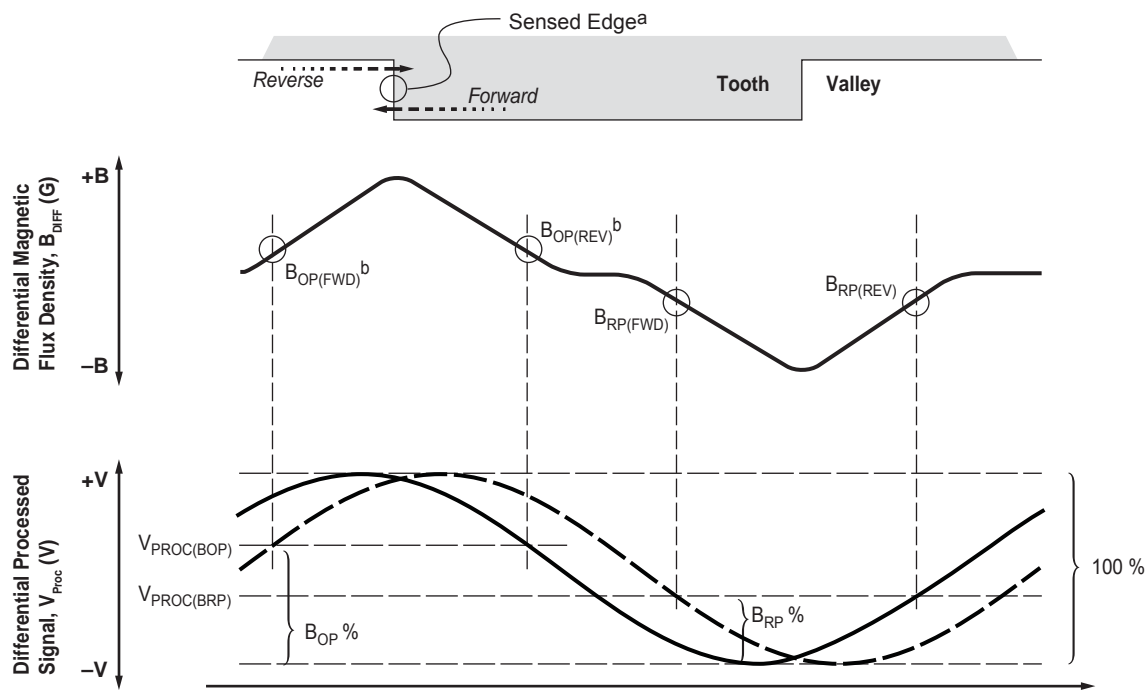
⁶Direction pulse will typically occur on the 2nd output pulse after a direction change. This will hold true unless an offset change at zero speed results in an offset correction event. Note that no output blanking occurs after a direction change.

⁷The device will compensate for magnetic and installation offsets up to $\pm 60 \text{ G}$. Offsets greater than $\pm 60 \text{ G}$ may cause inaccuracies in the output.

OPERATING CHARACTERISTICS: Switchpoint Characteristics Valid over operating voltage and temperature ranges, unless otherwise noted (refer to figure below)

Characteristics	Symbol	Test Conditions	Min.	Typ.	Max.	Unit
Target Frequency, Forward Rotation	f_{FWD}		–	–	12	kHz
Target Frequency, Reverse Rotation	f_{REV}		–	–	6	kHz
Target Frequency, Non-Direction Pulses*	f_{ND}		–	–	4	kHz
Bandwidth	f_{-3dB}	Cutoff frequency for low-pass filter	15	20	–	kHz
Operate Point	B_{OP}	% of peak-to-peak V_{PROC} referenced from PDAC to NDAC, $AG < AG_{max}$	–	70	–	%
Release Point	B_{RP}	% of peak-to-peak V_{PROC} referenced from PDAC to NDAC, $AG < AG_{max}$	–	30	–	%

*At power-on, rotational speed or vibration leading to a target frequency greater than 4 kHz may result in a constant high output state until true direction is detected.



^aSensed Edge: leading (rising) edge in forward rotation, trailing (falling) edge in reverse rotation

^b $B_{OP(FWD)}$ triggers the output pulse during forward rotation, and $B_{OP(REV)}$ triggers the output pulse during reverse rotation

OPERATING CHARACTERISTICS: Output Pulse Characteristics* Valid over operating temperature range, unless otherwise noted

Characteristics	Symbol	Test Conditions	Min.	Typ.	Max.	Unit
Pulse Width, Forward Rotation	$t_{w(FWD)}$	$R_L = 500 \Omega$, $C_L = 10 \text{ pF}$	38	45	52	μs
Pulse Width, Reverse Rotation	$t_{w(REV)}$	$R_L = 500 \Omega$, $C_L = 10 \text{ pF}$	76	90	104	μs
Pulse Width, Non-Direction	$t_{w(ND)}$	$R_L = 500 \Omega$, $C_L = 10 \text{ pF}$	153	180	207	μs

*Measured at a threshold of $(I_{CC(HIGH)} + I_{CC(LOW)}) / 2$.

OPERATING CHARACTERISTICS: Input Characteristics Valid over operating temperature range and using Reference Target 60-0, unless otherwise noted

Characteristics	Symbol	Test Conditions	Min.	Typ.	Max.	Unit
Operating Input Range ¹	B_{DIFF}	Differential magnetic signal; correct direction output on 6 th edge	60	–	1200	G
Maximum Operation Air Gap ¹	AG_{max}	Correct direction output on 6 th edge	–	–	2.2	mm
Vibration Immunity (Startup)	$Err_{VIB(SU)}$	Allowed rotation undetected due to vibration; T_{TOOTH} = period between 2 successive sensed edges, sinusoidal signal; $\Delta T_A < 10^\circ C$	T_{TOOTH}	–	–	–
Vibration Immunity (Running mode) ²	Err_{VIB}	Allowed rotation undetected due to vibration; T_{TOOTH} = period between 2 successive sensed edges, sinusoidal signal; $\Delta T_A < 10^\circ C$	$T_{TOOTH} \times 0.5$	–	–	–
Maximum Sudden Air Gap Change Induced Signal Reduction ^{3,4}	$\Delta B_{DIFF(AG)}$	Differential magnetic signal reduction due to instantaneous air gap change; symmetrical signal reduction, target frequency < 500 Hz	–	–	40	% _{pk-pk}
Axial/Radial Runout / Wobble Induced Signal Reduction ^{5,6}	$\Delta B_{DIFF(RO)}$	Differential magnetic signal reduction due to instantaneous runout per edge; symmetrical signal reduction, multiple edges	–	–	5	% _{pk-pk}
Relative Repeatability ⁷	$T_{\theta E}$	Differential magnetic signal, $B_{DIFF} = 100 G_{pk-pk}$, ideal sinusoidal signal, $T_A = 150^\circ C$, Reference Target rotational speed = 1000 rpm ($f = 1000$ Hz)	–	0.12	–	deg.
Switchpoint Margin	$V_{SP(margin)}$	Minimum separation between channels as a percentage of V_{PROC} amplitude at each switchpoint (see figure below)	20	–	160	% _{pk-pk}

¹Under certain extreme conditions, especially for smaller differential magnetic signals, the device may require more than 6 edges to output correct direction on startup. Please contact the Allegro factory for assistance when using this device.

²Small amplitude vibration while in Running mode may result in one additional direction pulse, prior to non-direction pulse. See section Running Small Amplitude Vibration Detection for details.

³If the minimum $V_{SP(margin)}$ is not maintained after a sudden air gap change, output may be blanked or non-direction pulses may occur.

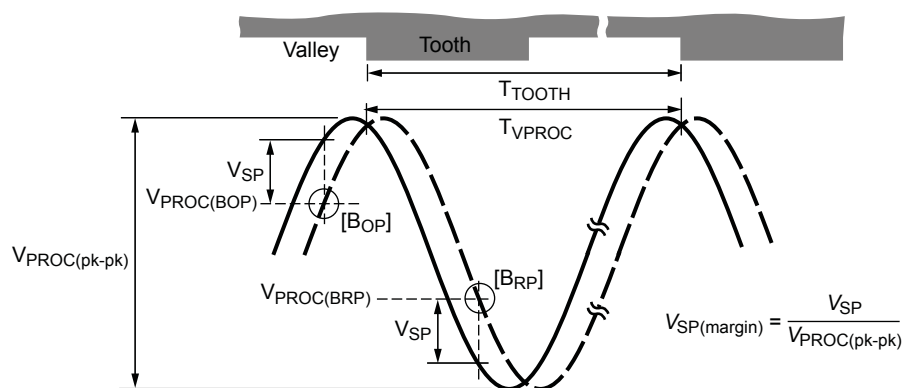
⁴Sudden air gap change during startup may increase the quantity of edges required to get correct direction pulses.

⁵If the minimum $V_{SP(margin)}$ is not maintained, output may be blanked or non-direction pulses may occur.

⁶Minimum $V_{PROC(pk-pk)}$ signal of 200 mV and minimum $V_{SP(margin)}$ must be maintained

⁷The repeatability specification is based on statistical evaluation of a sample population, evaluated at 1000 Hz.

Definition of Terms for Input Characteristics

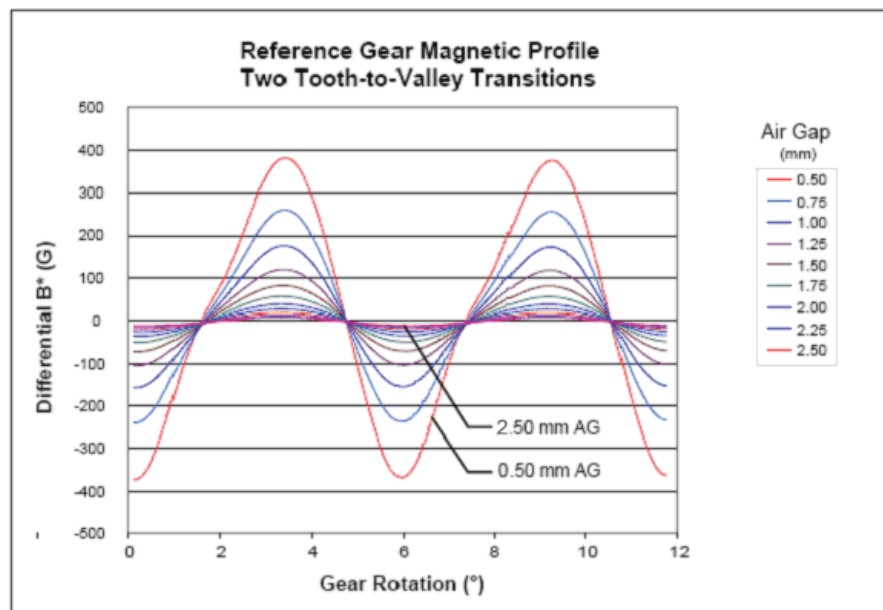
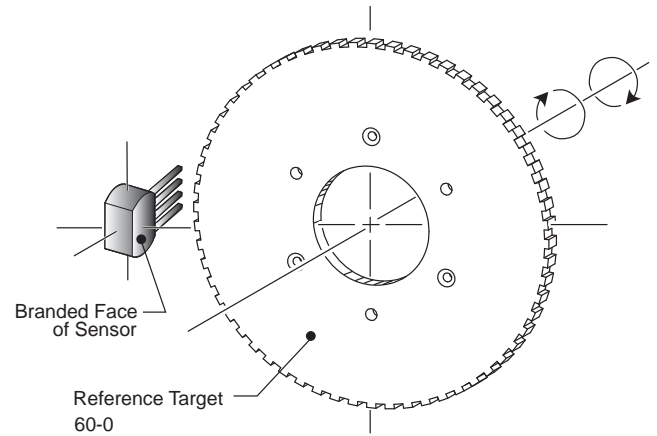
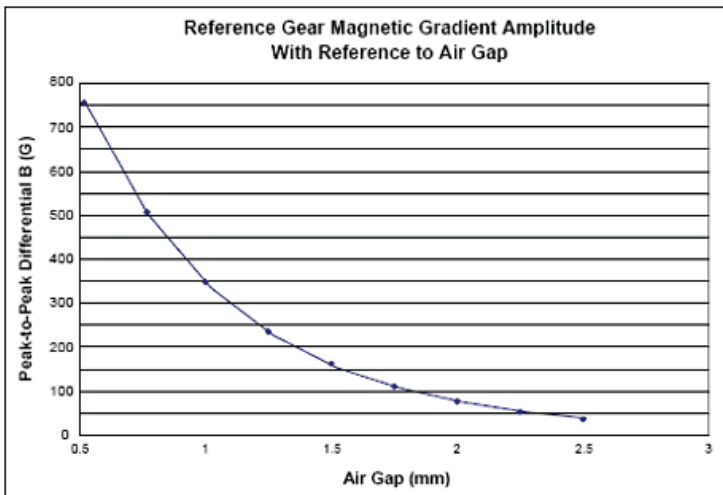


V_{PROC} = the processed analog signal of the sinusoidal magnetic input (per channel)

T_{tooth} = period of 2 successive sensed target edges

Reference Target 60-0 (60 Tooth Target)

Characteristics	Symbol	Test Conditions	Typ.	Units	Symbol Key
Outside Diameter	D_o	Outside diameter of target	120	mm	
Face Width	F	Breadth of tooth, with respect to sensor	6	mm	
Angular Tooth Thickness	t	Length of tooth, with respect to sensor	3	deg.	
Angular Valley Thickness	t_v	Length of valley, with respect to sensor	3	deg.	
Tooth Whole Depth	h_t		3	mm	
Material		Low Carbon Steel	-	-	



Functional Description

Data Protocol Description

When a target passes in front of the sensor (the branded face of the sensor case), each tooth of the target generates a pulse at the output pin of the sensor. Each pulse provides target speed and direction data: speed is provided by the pulse rate, while direction of target rotation is provided by the pulse width.

The ATS657 can sense target movement in both the forward and reverse directions. The maximum allowable target rotational speed is limited by the width of the output pulse and the shortest low-state duration the system controller can resolve.

Forward Rotation (see panel A in figure 1) When the target is rotating such that a tooth near the sensor passes from pin 4 to pin 1, this is referred to as *forward rotation*. Forward rotation is indicated on the output pin by a $t_{w(FWD)}$ (45 μs typical) pulse width.

Reverse Rotation (see panel B in figure 1) When the target is rotating such that a tooth passes from pin 1 to pin 4, it is referred to as *reverse rotation*. Reverse rotation is indicated on the output pulse

by a $t_{w(REV)}$ (90 μs typical) pulse width, twice as long as the pulse generated by forward rotation.

Timing As shown in figure 2, the pulse appears at the output pin slightly before the sensed magnetic edge traverses the sensor. For targets in forward rotation, this shift, Δfwd , results in the pulse corresponding to the valley with the sensed mechanical edge, and for targets in reverse rotation, the shift, Δrev , results in the pulse corresponding to the tooth with the sensed edge. The sensed mechanical edge that stimulates output pulses is kept the same for both forward and reverse rotation by using only channel 1 for switching.

The overall range between the forward and reverse pulse occurrences is determined by the 1.5 mm spacing between the Hall elements of the corresponding differential channel. In either direction, the pulses appear close to the sensed mechanical edge. The size of the target features, however, can slightly bias the occurrence of the pulses.

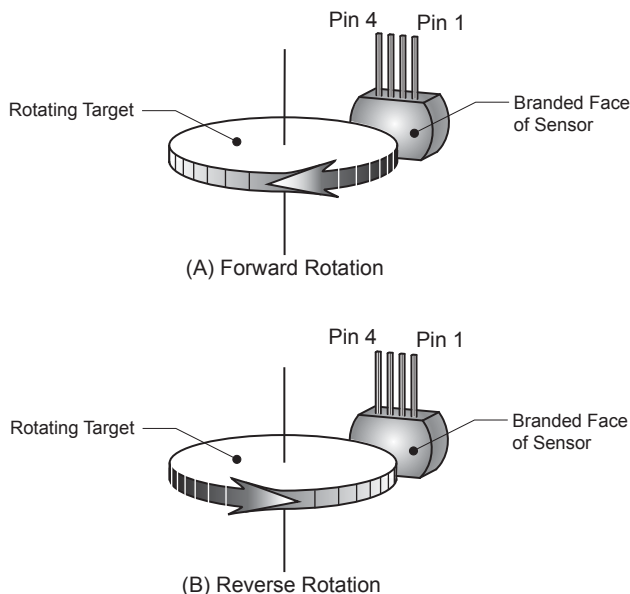


Figure 1. Target rotation

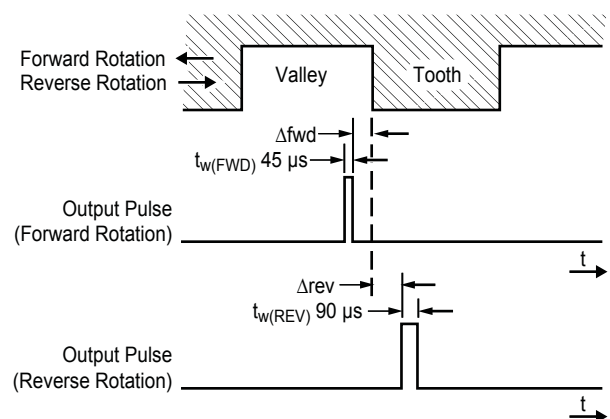


Figure 2. Output pulse timing

Start-Up Detection

After the power-on time is complete, the ATS657 internally detects the profile of the target. The output becomes active at the first detected switchpoint. Figure 3 shows where the first output

pulse occurs for various starting target phases. After calibration is complete, direction information is available and this information is communicated through the output pulse width.

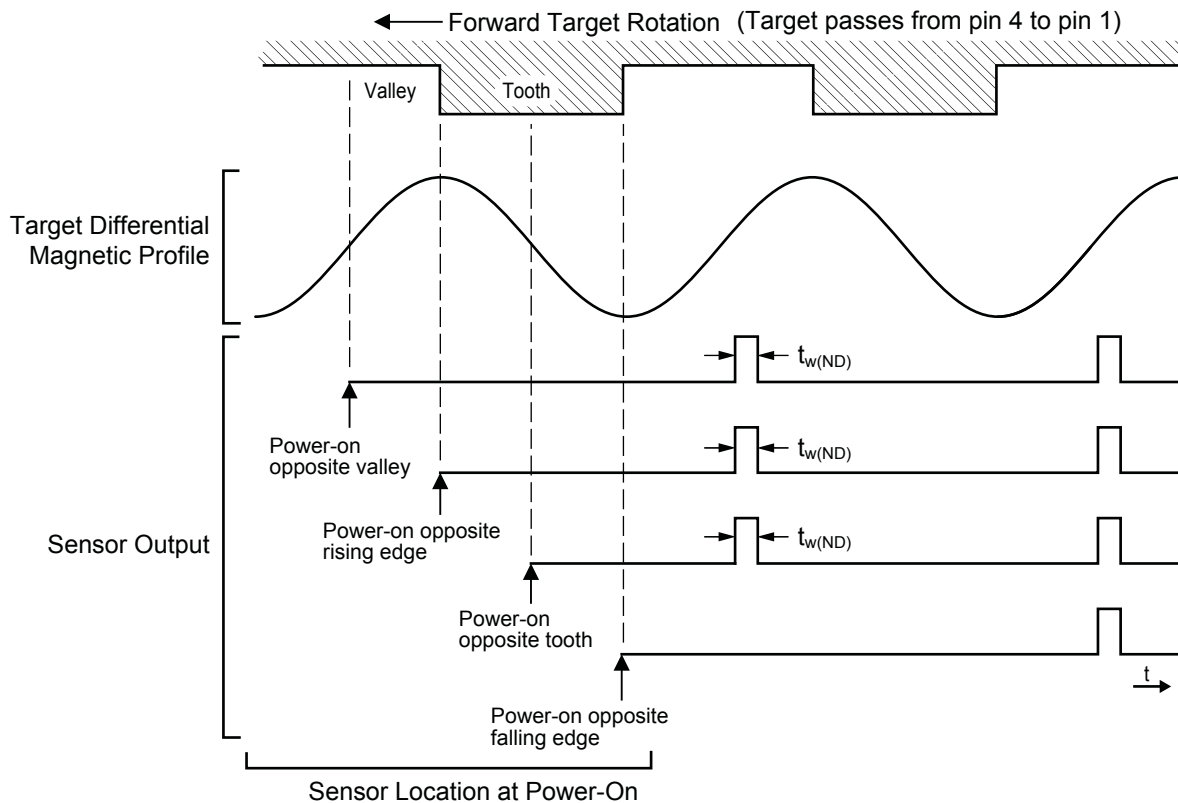


Figure 3. Start-up position effect on first device output switching

Continuous Update of Switchpoints

The processed differential internal analog signal, V_{PROC} , of each of the two channels is used to determine switchpoints, at which the device determines direction information and changes to output signal polarity. Because the value of V_{PROC} is directly proportional to the differential magnetic flux density, B_{DIFF} , induced by the target and sensed by the Hall elements, the switchpoints occur at threshold levels that correspond to certain levels of B_{DIFF} .

The *operate point*, B_{OP} , occurs when V_{PROC} rises through a certain limit, $V_{PROC(BOP)}$. When B_{OP} occurs, the channel internally switches from low to high. When V_{PROC} falls below $V_{PROC(BOP)}$ through a certain limit, $V_{PROC(BRP)}$, the *release point*, B_{RP} ,

occurs and the channel state switches from high to low.

As shown in panel C of figure 4, the threshold levels for the ATS657 switchpoints are established as a function of the two previous signal peaks detected. The ATS657 incorporates an algorithm that continuously monitors V_{PROC} and then updates the switching thresholds to correspond to any amplitude reduction. For any given target edge transition, the change in threshold level is limited. Each channel operates in this manner, independent of each other, so independent switchpoint thresholds are calculated for each channel.

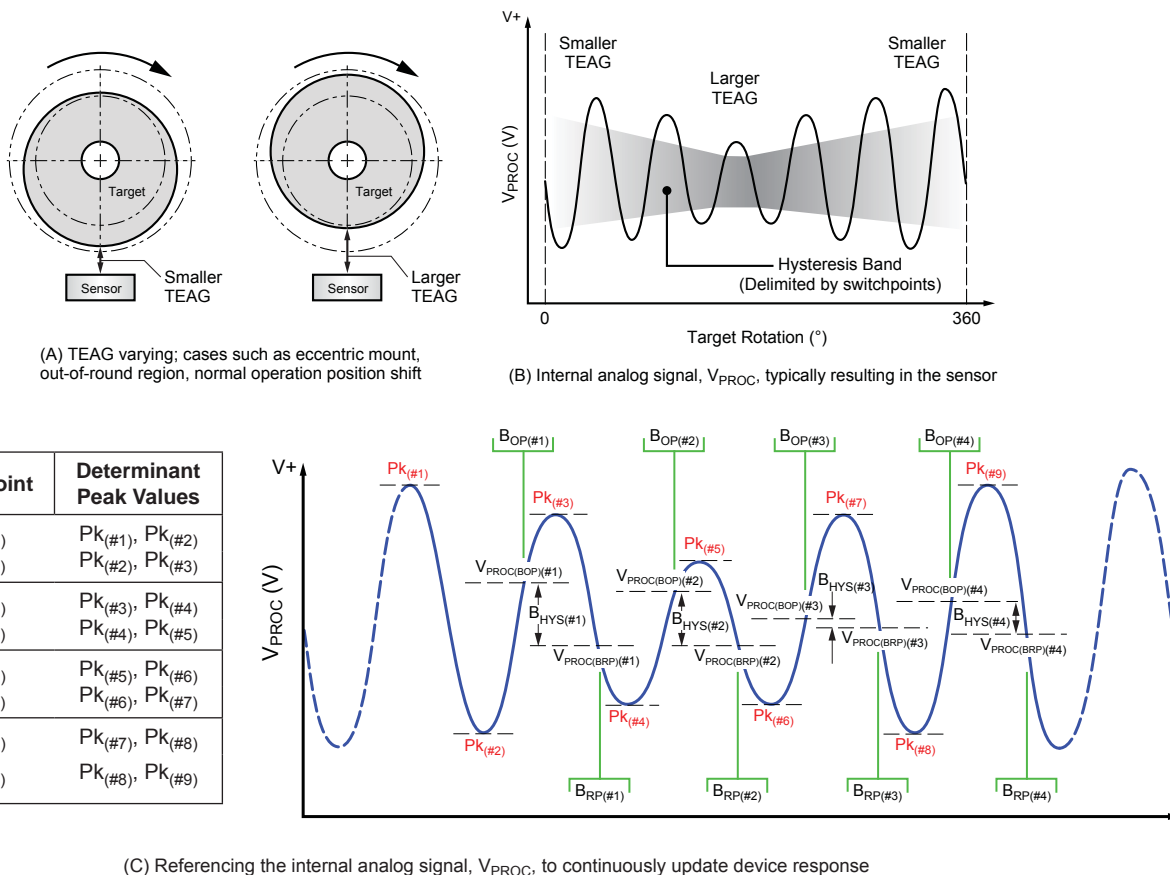


Figure 4. The Continuous Update algorithm allows the Allegro sensor to immediately interpret and adapt to variances in the magnetic field generated by the target as a result of eccentric mounting of the target, out-of-round target shape, elevation due to lubricant build-up in journal gears, and similar dynamic application problems that affect the TEAG (Total Effective Air Gap). Not detailed in the figure are the boundaries for peak capture DAC movement which intentionally limit the amount of internal signal variation the sensor is able to react to over a single transition. The algorithm is used to dynamically establish and subsequently update the device switchpoint levels ($V_{PROC(BOP)}$ and $V_{PROC(BRP)}$). The hysteresis, $B_{HYS}(\#x)$, at each target feature configuration results from this recalibration, ensuring that it remains properly proportioned and centered within the peak-to-peak range of the internal analog signal, V_{PROC} .

As shown in panel A, the variance in the target position results in a change in the TEAG. This affects the sensor as a varying magnetic field, which results in proportional changes in the internal analog signal, V_{PROC} , shown in panel B. The Continuous Update algorithm is used to establish accurate switchpoint levels based on the fluctuation of V_{PROC} , as shown in panel C.

Operation During Running Mode Vibration

During normal running mode, vibration can interfere with the direction detection functions. In that case, during the vibration the device continues to output speed data with non-directional pulses.

If the vibration that occurs has a high enough amplitude such that the peaks of the V_{PROC} signals continue to pass through both switchpoints, non-direction pulses will be outputted during the vibration, as shown in figure 5.

If the vibration has a low enough amplitude such that its posi-

tive peak is less than $V_{PROC(BOP)}$, no pulses are outputted and no switchpoint updating occurs until the vibration becomes large enough that V_{PROC} exceeds $V_{PROC(BOP)}$. If its negative peak is greater than $V_{PROC(BRP)}$, then there is no output or update until V_{PROC} falls below $V_{PROC(BOP)}$. As shown in figure 6, when that does occur, a single direction pulse may be outputted, however, regardless of whether or not that single pulse occurs, non-direction pulses are outputted throughout the remainder of the vibration.

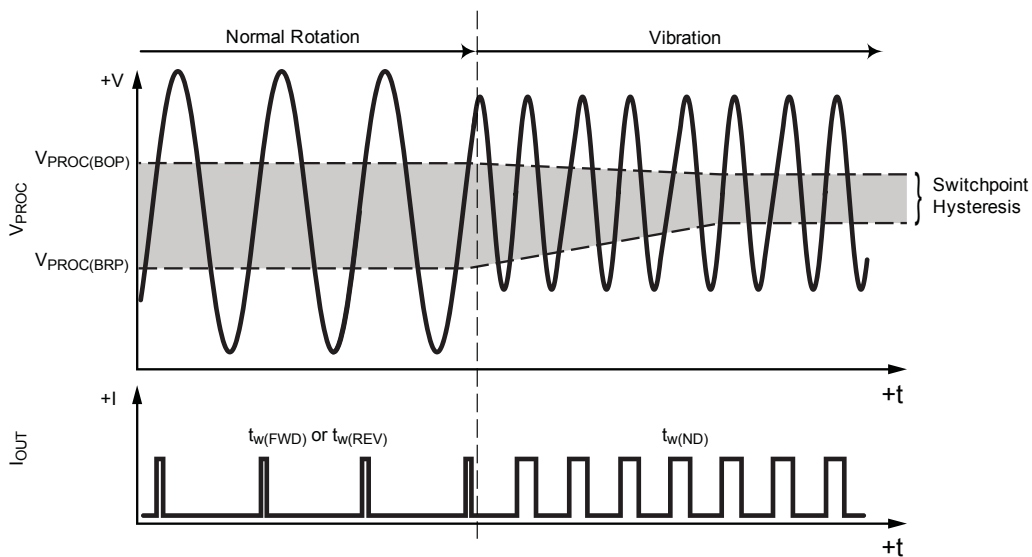


Figure 5. Large amplitude vibration during Running mode operation

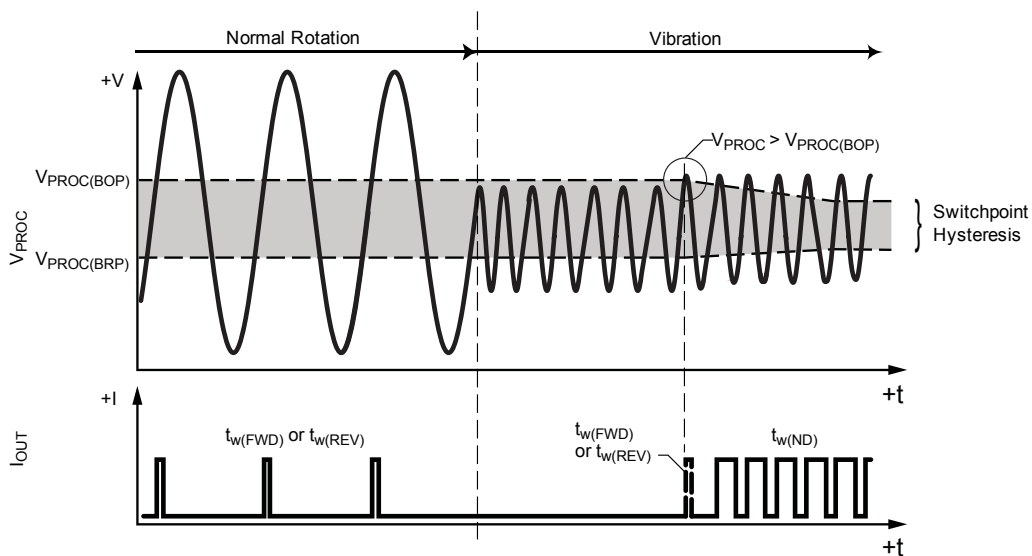


Figure 6. Small amplitude vibration during Running mode operation

Undervoltage Lockout

When the supply voltage falls below the minimum operating voltage, $V_{CC(UV)}$, I_{CC} goes low and remains low regardless of the state of the magnetic gradient from the target. This lockout feature prevents false signals, caused by undervoltage conditions, from propagating to the output of the sensor. I_{CC} levels may not meet datasheet limits when $V_{CC} < V_{CC(min)}$.

Power Supply Protection

The device contains an on-chip regulator and can operate over a wide V_{CC} range. For devices that need to operate from an unregulated power supply, transient protection must be added externally. For applications using a regulated line, EMI/RFI protection may still be required. Contact Allegro for information on the circuitry needed for compliance with various EMC specifications. Refer to figure 7 for an example of a basic application circuit.

Automatic Gain Control (AGC)

This feature allows the device to operate with an optimal internal electrical signal, regardless of the air gap (within the AG specification). At power-on, the device determines the peak-to-peak amplitude of the signal generated by the target. The gain of the sensor is then automatically adjusted. Figure 8 illustrates the effect of this feature. The two differential channels have their gain set independent of each other, so both channels may or may not have the same gain setting.

Automatic Offset Adjust (AOA)

The AOA circuitry, when combined with AGC, automatically compensates for the effects of chip, magnet, and installation offsets. (For capability, see Allowable User Induced Differential Offset, in the Electrical Characteristics table.) This circuitry is continuously active, including both during Power-On mode and Running mode, compensating for offset drift. Continuous operation also allows it to compensate for offsets induced by temperature variations over time. Similar to AGC, the AOA is set independently for each channel, so the offset adjust is set per channel, based on the offset characteristics of that specific channel.

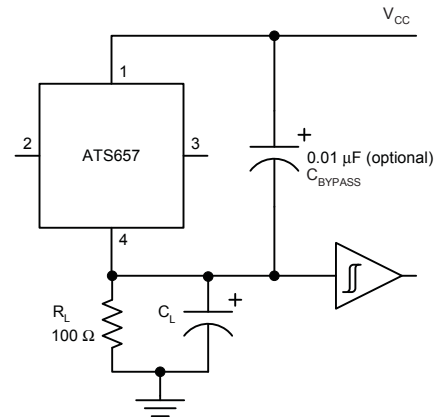


Figure 7. Typical application circuit

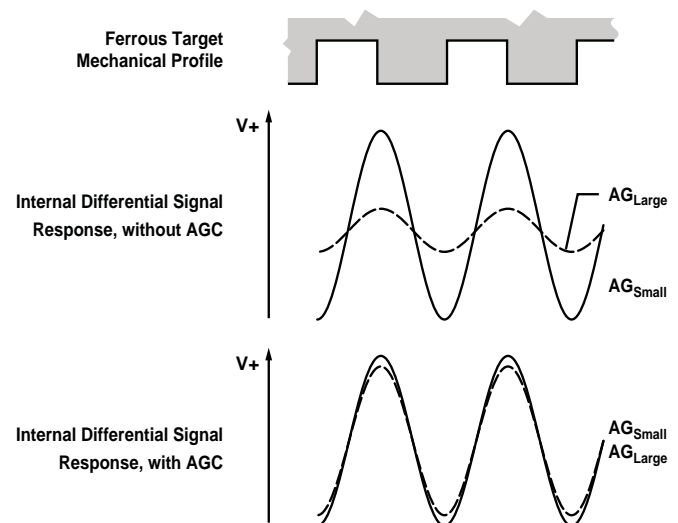
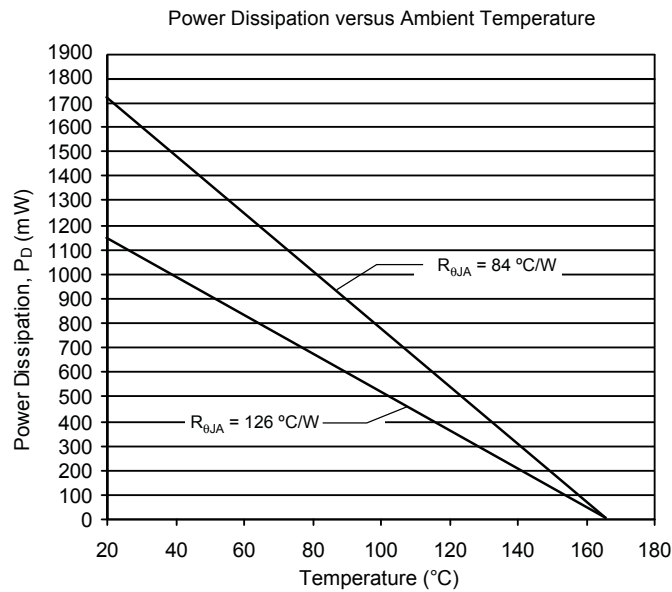
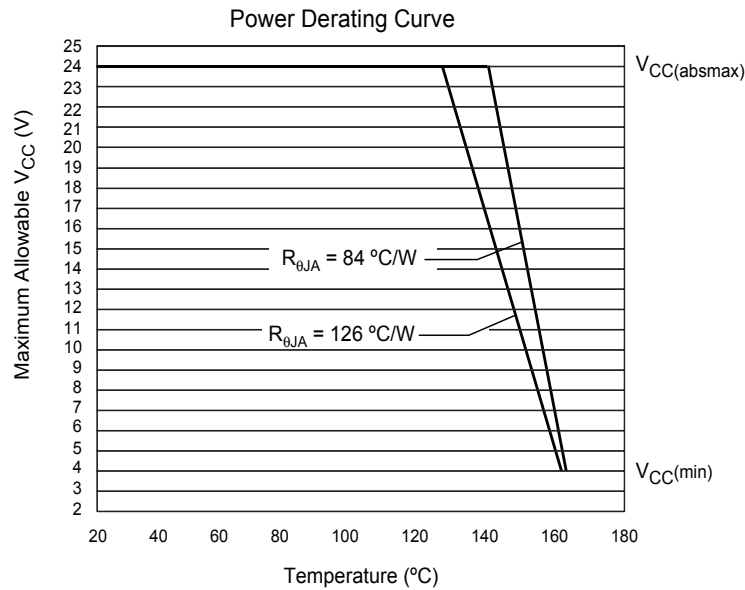


Figure 8. Automatic Gain Control (AGC). The AGC function corrects for variances in the air gap. Differences in the air gap cause differences in the magnetic field at the device, but AGC prevents that from affecting device performance, as shown in the lowest panel.

Thermal Characteristics may require derating at maximum conditions, see Power Derating section

Characteristic	Symbol	Test Conditions*	Value	Unit
Package Thermal Resistance	$R_{\theta JA}$	Single layer PCB, with copper limited to solder pads	126	$^{\circ}\text{C}/\text{W}$
		Single layer PCB, with limited to solder pads and 3.57 in. ² (23.03 cm ²) copper area each side	84	$^{\circ}\text{C}/\text{W}$

*Additional thermal information available on the Allegro website



Power Derating

The device must be operated below the maximum junction temperature of the device, $T_J(\text{max})$. Under certain combinations of peak conditions, reliable operation may require derating supplied power or improving the heat dissipation properties of the application. This section presents a procedure for correlating factors affecting operating T_J . (Thermal data is also available on the Allegro MicroSystems Web site.)

The Package Thermal Resistance, $R_{\theta JA}$, is a figure of merit summarizing the ability of the application and the device to dissipate heat from the junction (die), through all paths to the ambient air. Its primary component is the Effective Thermal Conductivity, K , of the printed circuit board, including adjacent devices and traces. Radiation from the die through the device case, $R_{\theta JC}$, is a relatively small component of $R_{\theta JA}$. Ambient air temperature, T_A , and air motion are significant external factors, damped by overmolding.

The effect of varying power levels (Power Dissipation, P_D), can be estimated. The following formulas represent the fundamental relationships used to estimate T_J , at P_D .

$$P_D = V_{IN} \times I_{IN}$$

$$\Delta T = P_D \times R_{\theta JA}$$

$$T_J = T_A + \Delta T$$

For example, given common conditions such as: $T_A = 25^\circ\text{C}$, $V_{CC} = 12\text{ V}$, $I_{CC} = 6.5\text{ mA}$, and $R_{\theta JA} = 126\text{ }^\circ\text{C/W}$, then:

$$P_D = V_{CC} \times I_{CC} = 12\text{ V} \times 6.5\text{ mA} = 78\text{ mW}$$

$$\Delta T = P_D \times R_{\theta JA} = 78\text{ mW} \times 126\text{ }^\circ\text{C/W} = 9.8^\circ\text{C}$$

$$T_J = T_A + \Delta T = 25^\circ\text{C} + 9.8^\circ\text{C} = 34.8^\circ\text{C}$$

A worst-case estimate, $P_D(\text{max})$, represents the maximum allowable power level ($V_{CC}(\text{max})$, $I_{CC}(\text{max})$), without exceeding $T_J(\text{max})$, at a selected $R_{\theta JA}$ and T_A .

Example: Reliability for V_{CC} at $T_A = 150^\circ\text{C}$, package SH, using single layer PCB.

Observe the worst-case ratings for the device, specifically: $R_{\theta JA} = 126^\circ\text{C/W}$, $T_J(\text{max}) = 165^\circ\text{C}$, $V_{CC(\text{absmax})} = 24\text{ V}$, and $I_{CC} = 13\text{ mA}$ (Note: At maximum target frequency, $I_{CC(\text{LOW})} = 8\text{ mA}$, $I_{CC(\text{HIGH})} = 16\text{ mA}$, and maximum pulse widths, the result is a duty cycle of 62.4% and a worst case mean I_{CC} of 13 mA.)

Calculate the maximum allowable power level, $P_D(\text{max})$. First, invert equation 3:

$$\Delta T(\text{max}) = T_J(\text{max}) - T_A = 165^\circ\text{C} - 150^\circ\text{C} = 15^\circ\text{C}$$

This provides the allowable increase to T_J resulting from internal power dissipation. Then, invert equation 2:

$$P_D(\text{max}) = \Delta T(\text{max}) \div R_{\theta JA} = 15^\circ\text{C} \div 126\text{ }^\circ\text{C/W} = 119\text{ mW}$$

Finally, invert equation 1 with respect to voltage:

$$V_{CC(\text{est})} = P_D(\text{max}) \div I_{CC} = 119\text{ mW} \div 13\text{ mA} = 9.2\text{ V}$$

The result indicates that, at T_A , the application and device can dissipate adequate amounts of heat at voltages $\leq V_{CC(\text{est})}$.

- (1) Compare $V_{CC(\text{est})}$ to $V_{CC(\text{max})}$. If $V_{CC(\text{est})} \leq V_{CC(\text{max})}$, then reliable operation between $V_{CC(\text{est})}$ and $V_{CC(\text{max})}$ requires enhanced $R_{\theta JA}$.
- (2) If $V_{CC(\text{est})} \geq V_{CC(\text{max})}$, then operation between $V_{CC(\text{est})}$ and $V_{CC(\text{max})}$ is reliable under these conditions.

Copyright ©2009, Allegro MicroSystems, Inc.

The products described herein are manufactured under one or more of the following U.S. patents: 5,045,920; 5,264,783; 5,442,283; 5,389,889; 5,581,179; 5,517,112; 5,619,137; 5,621,319; 5,650,719; 5,686,894; 5,694,038; 5,729,130; 5,917,320; and other patents pending.

Allegro MicroSystems, Inc. reserves the right to make, from time to time, such departures from the detail specifications as may be required to permit improvements in the performance, reliability, or manufacturability of its products. Before placing an order, the user is cautioned to verify that the information being relied upon is current.

Allegro's products are not to be used in life support devices or systems, if a failure of an Allegro product can reasonably be expected to cause the failure of that life support device or system, or to affect the safety or effectiveness of that device or system.

The information included herein is believed to be accurate and reliable. However, Allegro MicroSystems, Inc. assumes no responsibility for its use; nor for any infringement of patents or other rights of third parties which may result from its use.

For the latest version of this document, visit our website:

www.allegromicro.com

